

Optical lever calibration in atomic force microscope with a mechanical lever

Hui Xie, Julien Vitard, Sinan Haliyo, and Stéphane Régnier

Institut des Systèmes Intelligents et Robotique (ISIR), Université Pierre et Marie Curie-Paris, 6/CNRS 18 Route du Panorama-BP 61, 92265 Fontenay-Aux-Roses, France

(Received 11 June 2008; accepted 3 August 2008; published online 4 September 2008)

A novel method that uses a small mechanical lever has been developed to directly calibrate the lateral sensitivity of the optical lever in the atomic force microscope (AFM). The mechanical lever can convert the translation into a nanoscale rotation angle with a flexible hinge that provides an accurate conversion between the photodiode voltage output and torsional angle of a cantilever. During the calibration, the cantilever is mounted on a holder attached on the lever, which brings the torsional axis of the cantilever and rotation axis of the lever into line. By making use of its nanomotion on the Z-axis and using an external motion on the barrier, this device can complete the local and full-range lateral sensitivity calibrations of the optical lever without modifying the actual AFM or the cantilevers. © 2008 American Institute of Physics. [DOI: 10.1063/1.2976108]

A great deal of attention has been paid to techniques for a reliable and precise calibration of the lateral force application in atomic force microscopes (AFMs) since the first friction force measurement with an AFM by Mate *et al.*¹ Two kinds of methods are commonly used in the lateral force calibration, a one-step method and a two-step method. The one-step method,^{2–9} bypassing difficulties in the separate measurement of the lateral stiffness of the cantilever and lateral sensitivity of the photodiode, directly determines the conversion factor between the lateral force and lateral photodiode response. The two-step method, which is similar to the normal force calibration, involves the calibration of the cantilever's torsional spring constant^{10–13} and the sensitivity of the lateral photodiode response. However, lateral sensitivity is more difficult to determine because the contact stiffness between the tip and the sample surface is proportional to the contact radius¹⁴ and is often comparable to the cantilever stiffness and the tip stiffness,¹⁵ which significantly reduces the calibration result of the photodiode's lateral sensitivity.^{16,17} In order to overcome this limitation, for example, the photodiode's lateral sensitivity was obtained by changing the position of the photodiode¹¹ or using a tilted mirror to measure the output voltage as a function of the angle.¹² Colloidal probes may be the most popular method used to achieve the lateral sensitivity measurement.^{16–18} Moreover, the full range of lateral photodiode sensitivity was successfully determined by loading the colloidal sphere laterally against a vertical sidewall.¹⁷ This is a significant step in the nonlinear compensation in the lateral force application.¹⁹ Overall, in the two-step method, the main obstacle in the lateral sensitivity calibration is the difficulty in determining the actual lateral deflection using the conventional displacement-voltage conversion between the tip displacement and photodiode output.

Here, we present a new method to calibrate the lateral sensitivity of the optical lever using a small mechanical lever with a flexible hinge. This device can directly transfer the lever translation into the angular deflection of any type of

cantilever mounted on the mechanical lever using a simple geometric calculation.

In the alternative method for the calibration of the lateral sensitivity of the photodiode response, a mechanical lever, fabricated by the electric discharging machining (EDM) technique, is used as a so-called translator for translation-to-angle conversion. A lever with dimensions of $22 \times 8 \times 4$ mm³ was used in our experiments. Simulation and experimental results indicate that its dimensions can be, in fact, reduced much to match space limitations of the AFM in actual use. A diagram of the experimental setup is shown in Figs. 1(a)–1(c). In Fig. 1(a), the mechanical lever is fixed on the AFM stage and a testing cantilever is mounted on a holder attached to the upper beam of the lever, deliberately bringing the torsional axis of the cantilever and rotation axis of the lever in line. When the AFM stage moves vertically with a displacement Δz , it pushes the mechanical lever against a barrier located on the top surface of the upper beam with a distance of L from the center of the flexible hinge, converting the translation into a nanoscale rotation of the upper beam of the lever [in Fig. 1(b)]. In this case, the accurate translation on the Z-axis of the AFM stage can be converted into a rotation on the cantilever, imitating a torsional deflection of the cantilever deduced by a torsional moment applied on it. In Fig. 1(c), a finite-element analysis of the displacement vector distribution of the upper beam shows that its rotation is nicely around the center of the flexible hinge when a displacement is applied on the lever's pan. This lever can accurately calibrate the lateral sensitivity of the photodiode response without any clearance or creep due to the flexible hinge used for a kinematic transform. More importantly, this method can be used to directly calibrate the sensitivities of any type of cantilevers mounted on the mechanical lever instead of a tilted reflecting mirror¹² and without any changes⁴ and load applied to the cantilevers, obtaining a nondestructive and more accurate conversion between the lateral angular deflection and the photodiode response.

As shown in Fig. 1(b), the geometric transform between the displacement Δz applied on the pan and the rotation

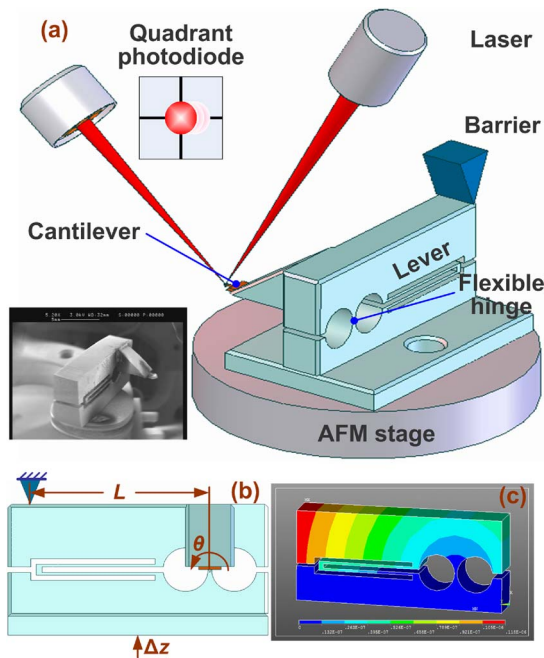


FIG. 1. (Color online) Diagram of the experimental setup. (a) A small mechanical lever with a flexible hinge. The inset shows a scanning electron microscope image of a mechanical lever ($15 \times 8 \times 4$ mm³) with an attached cantilever. (b) The geometric transform between the AFM stage displacement Δz and a rotation angle θ of the cantilever. (c) Finite-element analysis of the displacement vector distribution of the upper beam.

angle $\Delta\varphi$ on the cantilever can be simplified as

$$\Delta\varphi = \frac{\Delta z}{L}, \quad (1)$$

where L is the distance between the barrier location and the center of the flexible hinge. Thus, when the voltage output V_l of the photodiode and the corresponding displacement Δz are known, the lateral angular sensitivity S_l of the photodiode can be easily obtained from Eq. (1) as

$$S_l = \frac{V_l}{\Delta\varphi} = \frac{V_l L}{\Delta z}. \quad (2)$$

The sensitivity of the photodiode response is strongly dependent on the position of the laser spot relative to the center of the position-sensitive detector (PSD),¹⁷ introducing nonlinearities of photodiode output due to the shape and intensity distribution of the laser spot on the PSD.²⁰ Thus, the local sensitivities of the photodiode were calibrated by adjusting the laser spot on different positions on the photodiode. Due to the limited range of the AFM stage, the motor-driven stage in our experiments was employed to push the barrier in full-range sensitivity characterization of the photodiode response. Moreover, the photodiode response significantly differs between cantilevers with different widths or surface coatings, which strongly relate to the intensity of the reflected laser on the photodiode.¹⁷ Therefore, further experiments were carried out to compare photodiode response using different types of cantilevers with various widths and reflectivities in their reflex coating.

After the mechanical lever was fixed on the AFM stage with a cantilever (ContAL, Budget Sensors) mounted on the

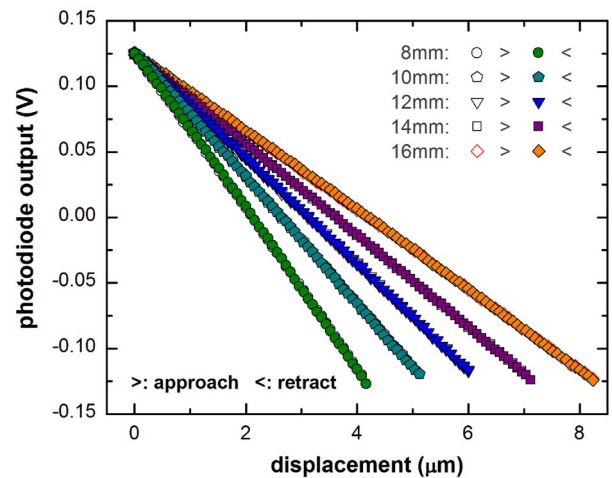


FIG. 2. (Color online) Examples of the sensitivity calibration results acquired using the developed mechanical lever with different locating positions of the barrier.

holder. The experiments described below were performed on a home-built AFM/optical nanomanipulation system under an ambient environment in the air.

In the local lateral sensitivity calibration, we translated the laser spot symmetrically around the center of the photodiode with the same range of photodiode outputs. In this case, the scanning displacements on different barrier loading positions were decided by

$$\Delta z = \frac{l}{l_0} \Delta z_0, \quad (3)$$

where l_0 is a reference position of the barrier with a photodiode response of about ± 120 mV deduced by the AFM stage displacement Δz_0 . In the experiments, $l_0 = 8$ mm was selected and $\Delta z_0 = 4$ μ m was decided accordingly.

In the experiments, ten loading positions (L) from 8 to 17 mm with an interval of 1 mm were used. Figure 2 shows examples of the local sensitivity calibration results obtained on five positions from 8 to 16 mm with an interval of 2 mm. Open and closed symbols refer to the approaching and retracting data, respectively. The data show that very small hysteresis loops occur between the approaching and retracting plots due to the closed loop control of the Z nanostage as well as the nonclearance and noncreep flexible hinges. Slopes of each of the plots are the photodiode voltage outputs versus displacements of the AFM stage, which can be easily converted into the lateral sensitivities by Eq. (2).

In Fig. 3(a), a full-range calibration result obtained on the 15 mm loading position is plotted. Open and closed circles refer to the approaching and retracting data, respectively. The hysteresis loop of these plots is due to the backlash of the motor-driven stage. Diamond symbols refer to the lateral full-range sensitivity calculated by making the derivative of the approaching data. A nonlinear fit using the Gauss function indicates that the calibrated result agrees well with the behavior predicted by Gaussian distribution of the laser spot positions on the photodiode. Another full-range sensitivity was also characterized by the local sensitivity calibration method by translating the photodiode laterally from the left- to the right-hand sides with an interval of 0.1 V in photodiode output and repeating the local sensitivity calibra-

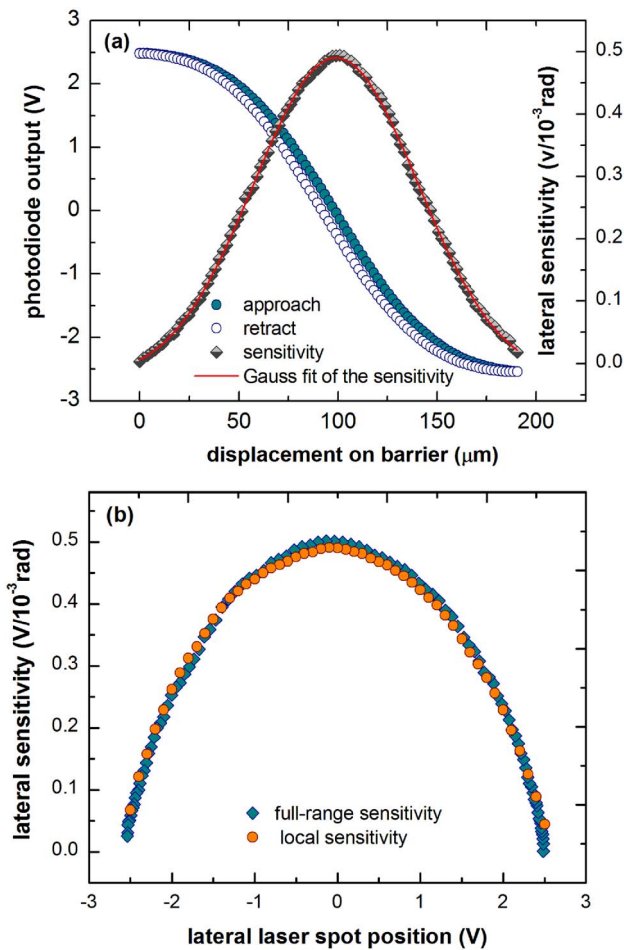


FIG. 3. (Color online) Full range calibration of the photodiode response. (a) Full response plot of the photodiode vs the barrier displacement on $L = 15$ mm. (b) Lateral sensitivity vs spot position plot on the photodiode obtained by the local and full-range calibration methods.

tion on each position, as shown in Fig. 3(b) by closed circles. For comparison, the full-range sensitivity obtained by the moving barrier is also plotted here by the diamond symbols. Small differences between these two methods (maximum difference on the photodiode center is about 0.011 V/10⁻³ rad, approximately 2.2% of the corresponding sensitivity). This difference may be due to the local sensitivity calibration, which averages the photodiode responses on neighboring ranges of each spot position.

Four types of cantilevers, including the cantilever used in the former experiments (termed tip 1 here) with the same reflex coating material (aluminum), were used in further experiments of the local sensitivity comparison on the photodiode center. Each type of cantilever is from the same batch packed in the same box with ten pieces. Figure 4 shows a comparison of the average sensitivities of these four types of cantilevers, in which the error bars show an overall error of $\pm 5.6\%$ of the sensitivities, which is deduced from uncertainties: $L: 0.2$ mm, $V_l: 0.015$ V, and $\Delta z: 5$ nm. The results show that the sensitivity is much more dependent on the reflex coating than the width of the cantilever. Great divergence of the reflectivity occurs due to the different properties of the reflex coating even when cantilevers have the same type of reflex coating and similar width. Therefore, it is nec-

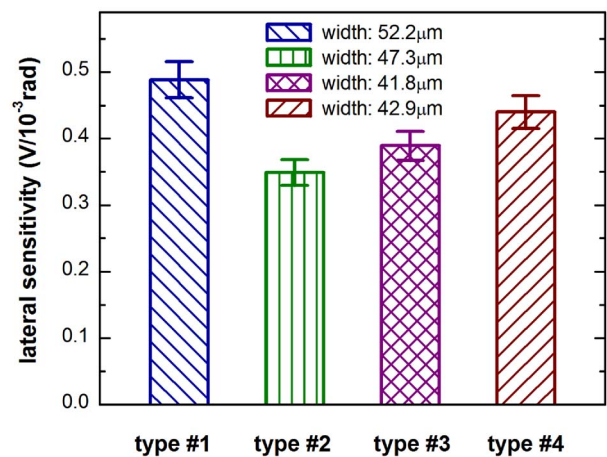


FIG. 4. (Color online) Lateral sensitivity calibration results using four types of cantilevers with the same aluminum coating and different widths.

essary to recalibrate the sensitivity when a different type of cantilever is used.

In summary, we have presented a new method to calibrate the lateral sensitivity of the optical lever in the AFM using a mechanical lever with a flexible hinge. In the experiments, small- and large-range scanings, respectively, were used to calibrate the local- and full-range sensitivities of the photodiode response, and the calibration results are accurate to $\pm 5.6\%$. A method such as this may allow accurate, direct, and nondestructive calibration of the lateral sensitivity of the optical lever in AFMs without any modification to the actual AFM or the cantilevers, thereby enabling an accurate calibration of the lateral force measurement in AFM.

- ¹C. M. Mate, G. M. McClelland, S. Chiang, and R. Erlandsson, *Phys. Rev. Lett.* **59**, 1942 (1987).
- ²D. F. Ogletree, R. W. Carpick, and M. Salmeron, *Rev. Sci. Instrum.* **67**, 3298 (1996).
- ³M. Varenberg, I. Etsion, and G. Halperin, *Rev. Sci. Instrum.* **74**, 3362 (2003).
- ⁴A. Feiler, P. Attard, and I. Larson, *Rev. Sci. Instrum.* **71**, 2746 (2000).
- ⁵N. Morel, M. Ramonda, and P. Tordjeman, *Appl. Phys. Lett.* **86**, 163103 (2005).
- ⁶W. H. Liu, K. Bonin, and M. Guthold, *Rev. Sci. Instrum.* **78**, 063707 (2007).
- ⁷P. J. Cumpson, J. Hedley, and C. A. Clifford, *J. Vac. Sci. Technol. B* **23**, 1992 (2005).
- ⁸Q. Li, K. S. Kim, and A. Rydberg, *Rev. Sci. Instrum.* **77**, 065105 (2006).
- ⁹H. Xie, J. Vitard, S. Haliyo, S. Régner, and M. Boukallel, *Rev. Sci. Instrum.* **79**, 033708 (2008).
- ¹⁰J. Neumeister and W. A. Ducker, *Rev. Sci. Instrum.* **65**, 2527 (1994).
- ¹¹E. Liu, B. Blanpain, and J. P. Celis, *Wear* **192**, 141 (1996).
- ¹²G. Bogdanovic, A. Meurk, and M. W. Rutland, *Colloids Surf., B* **19**, 397 (2000).
- ¹³S. Jeon, Y. Braiman, and T. Thundat, *Appl. Phys. Lett.* **84**, 1795 (2004).
- ¹⁴R. W. Carpick, D. F. Ogletree, and M. Salmeron, *Appl. Phys. Lett.* **70**, 1548 (1997).
- ¹⁵M. A. Lantz, S. J. O'shea, A. C. F. Hoole, and M. E. Welland, *Appl. Phys. Lett.* **70**, 970 (1997).
- ¹⁶R. G. Cain, S. Biggs, and N. W. Page, *J. Colloid Interface Sci.* **227**, 55 (2000).
- ¹⁷R. J. Cannara, M. Eglin, and R. W. Carpick, *Rev. Sci. Instrum.* **77**, 053701 (2006).
- ¹⁸S. Ecke, R. Raiteri, E. Bonaccorso, C. Reiner, H. J. Deiseroth, and H. J. Butt, *Rev. Sci. Instrum.* **72**, 4164 (2001).
- ¹⁹H. Xie, J. Vitard, S. Haliyo, and S. Régner, *IEEE Sens. J.* **8**, 1478 (2008).
- ²⁰T. E. Schaffer and P. R. Hansma, *J. Appl. Phys.* **84**, 4661 (1998).